Hindawi
International Journal of Spectroscopy
Volume 2017, Article ID 1614654, 9 pages
https://doi.org/10.1155/2017/1614654

Research Article

Determination of Metals Present in Textile Dyes Using Laser-Induced Breakdown Spectroscopy and Cross-Validation Using Inductively Coupled Plasma/Atomic Emission Spectroscopy

K. Rehan,[1,2,3] I. Rehan,[3] S. Sultana,[4] M. Zubair Khan,[3] Z. Farooq,[5] A. Mateen,[2] and M. Humayun[6]

[1]*State Key Laboratory of Magnetic Resonance and Atomic and Molecular Physics, Wuhan Institute of Physics and Mathematics, Chinese Academy of Sciences, Wuhan 430071, China*
[2]*The World Academy of Sciences (TWAS), Trieste, Italy*
[3]*Department of Applied Physics, Federal Urdu University of Arts, Science and Technology, Islamabad 44000, Pakistan*
[4]*Department of Chemistry, Islamia College University, Peshawar 25120, Pakistan*
[5]*Department of Physics, Quaid-i-Azam University, Islamabad 45320, Pakistan*
[6]*Department of Basic Sciences, University of Engineering and Technology, Peshawar 25120, Pakistan*

Correspondence should be addressed to I. Rehan; irehanyousafzai@gmail.com

Received 16 March 2017; Revised 7 June 2017; Accepted 16 July 2017; Published 28 August 2017

Academic Editor: Jozef Kaiser

Laser-induced breakdown spectroscopy (LIBS) was used for the quantitative analysis of elements present in textile dyes at ambient pressure via the fundamental mode (1064 nm) of a Nd:YAG pulsed laser. Three samples were collected for this purpose. Spectra of textile dyes were acquired using an HR spectrometer (LIBS2000+, Ocean Optics, Inc.) having an optical resolution of 0.06 nm in the spectral range of 200 to 720 nm. Toxic metals like Cr, Cu, Fe, Ni, and Zn along with other elements like Al, Mg, Ca, and Na were revealed to exist in the samples. The %-age concentrations of the detected elements were measured by means of standard calibration curve method, intensities of every emission from every species, and calibration-free (CF) LIBS approach. Only Sample 3 was found to contain heavy metals like Cr, Cu, and Ni above the prescribed limit. The results using LIBS were found to be in good agreement when compared to outcomes of inductively coupled plasma/atomic emission spectroscopy (ICP/AES).

1. Introduction

Laser-induced breakdown spectroscopy provides an easy, swift, and real-time elemental study, with no or very little preparation of samples. The rapid increase in applications of LIBS is due to the continuous research and advancements in the fields of lasers, optics, and related photodetectors [1–6]. Applications of LIBS are increasing rapidly in different fields, such as in environmental applications, in health [7, 8], in soil, and in energetic and biochemical investigations [9, 10]. When an intense laser beam, having power density greater than the threshold value of the sample surface, is focused onto the surface of a target, plasma is generated due to high temperature and pressure. The spectral emission from the laser generated plasma is used as a fingerprint wavelength, which assists the detection of the elemental composition of the target. In 2016, CF-LIBS approach was employed for the determination of elemental contents in potatoes [11]. This technique was successfully applied to measure the amount of minerals and toxic metals in calcified tissues [12]. A pulsed Nd:YAG laser was applied to carry out elemental analysis of aluminum alloys [13]. LIBS was applied to analyze edible salts appropriate for patients with kidney problems [14]. The same method was used for the quantitative determination of toxic metals in paints and the measurements are compared with the results of inductively coupled plasma (ICP) spectroscopy [15].

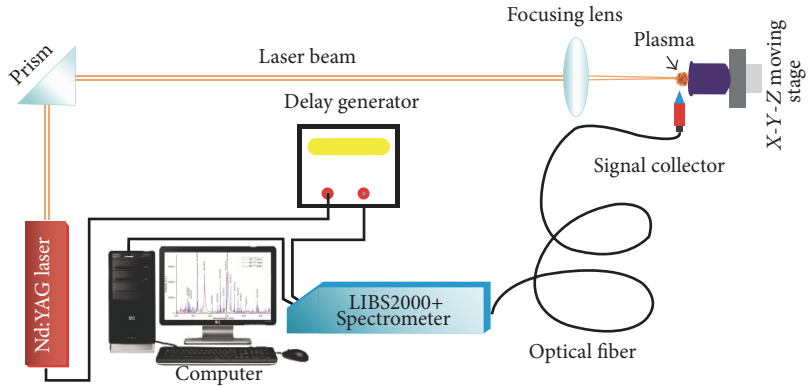

Figure 1: Experimental setup used in the present study.

Elemental determination of iron slag samples has been successfully investigated with the methodology we used in the current research work [16]. The elemental determination of pollutants in soils such as chromium, copper, lead, vanadium, and zinc has been carried out using LIBS [17], and similarly LIBS was also utilized for the quantitative and depth profiling study of Cu(In, Ga) Se_2 thin films [18].

The aim of the current study is to apply LIBS to analyze elements (including heavy and other elements) and their relative abundance in textile dyes in Pakistan, as it is observed that textile dyes containing toxic metals may cause health risks to clients such as allergic problems in particular. Moreover, quantitative measurement of metal contents can be also useful in a sense that some toxic elements present in dyes may cause problems to workers during their production phase.

Three samples of textile dyes were purchased from a local market in Rawalpindi city of Pakistan, namely, Sample 1 (red dye), Sample 2 (green dye), and Sample 3 (black dye). After separately crushing the samples to powder form, every sample was converted to pellet form. 10 gm of the homogeneous sample was placed in a cylindrical die and pressed hard by applying a load of 10 tons for 30 minutes to make the pellets. These pellets were pasted on a moveable stand and the laser was focused on their surfaces to generate the plasma and the associated emission spectra. To evaluate the %-age concentrations of the observed elements in the dyes, three different techniques based on LIBS were used, namely, standard calibration curve method, intensities of every emission from every species, and calibration-free LIBS approach. The comparative analysis between the results and the outcomes using ICP/atomic emission spectroscopy was carried out and was found to be in excellent harmony. Particularly, Sample 3 was observed to be composed of toxic metals like Cr, Cu, and Ni above the permissible limit that may be hazardous to consumers.

2. Experimental Setup

The schematic arrangement of LIBS experimental setup used in our study is illustrated in Figure 1. A pulsed laser from a Q-switched Nd:YAG laser (Ocean Optics, Inc.) working at 1064 nm, 5 ns pulsed duration, and 10 Hz repetition rate was utilized to create the plasma. Gate delay was 2 μs, and the integration time/gate width was selected as 3 ms. This laser is capable of delivering energy up to 400 mJ at 1064 nm. A calibrated energy meter (NOVA-QTL, P/N 1Z01507, sr. number 56461) was engaged to measure the pulsed energy. The laser beam was focused on the surface of the sample placed on target stand through a focusing lens (f = of 200 mm). The target was pasted on a rotating target stand, which was gradually rotating at a rate of ~5 mm/sec to provide a fresh surface after every laser shot in order to keep away from drilling on the target surfaces. The laser energy was optimized to 100 mJ/pulse. To avoid air breakdown in front of the sample, the distance of the focusing lens to the sample was adjusted as 180 mm. An HR spectrometer (LIBS2000+, Ocean Optics, Inc.) detection system with an optical resolution of 0.06 nm in combination with a collecting fiber (high OH, core diameter: 600 μm) of a collimating lens (0°–45° field of view) was used to register the spectral emissions from the plasma plume. The spectral emissions were collected by a collecting lens placed at 90° to the direction of plume expansion and the system was optimized for the background noise.

The OOILIBS software was used to subtract the background noise of the detector prior to analysis. The LIBS2000+ detection system was outfitted with five HR spectrometers; every one of them had 5 μm slit width and 2048-element linear CCD array. The spectrometer (Ocean Optics, Inc.) covers the spectral range of 220–720 nm. The LIBS2000+ detector and the Nd:YAG pulsed laser were synchronized to register the emission spectrum from the plume. The Q-switch and laser pulsed energy were varied using built-in software OOILIBS. The data recorded via five miniature spectrometers of the LIBS2000+ system was stored in a computer for further investigation.

For ICP analysis of the textile dyes, the samples were ground to powder, and 1/2 g of the samples was digested in strong HNO_3 and left for 24 hr. 10 mm of $HClO_4$ was mixed and the mixture was then heated at a temperature of 280 to 300°C. While heating, 2-3 mL of H_2O_2 was added slowly until the appearance of a transparent solution. Afterwards, the samples were diluted up to 50 mL with HNO_3 (3%) and then cleaned via a filter paper. The resultant remainder was studied by ICP/AES (Optima 2100-DV; Dual View, PerkinElmer).

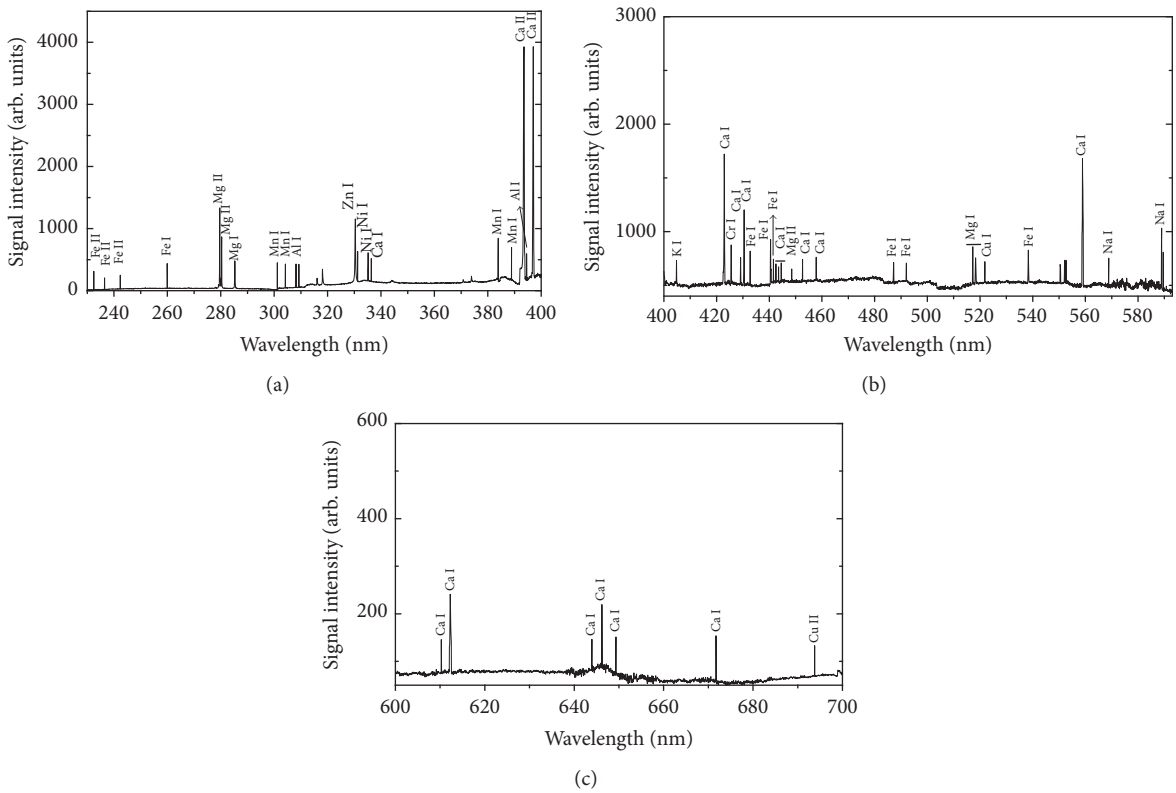

Figure 2: LIBS emission spectrum of textile dye (Sample 1) covering the spectral range 220–700 nm at ambient environment using 1064 nm pulses of Nd:YAG laser.

Table 1: Instrumental parameters for ICP/AES.

Detector	Solid state detector
Operating power (watt)	1300
Sample flow rate (mL min^{-1})	1.50
Nebulizer gas flow (L min^{-1})	0.80
Plasma gas flow (L min^{-1})	15.0
Supporting gas flow (L min^{-1})	0.2

Table 1 displays the parameters of ICP spectrometer used during this study.

3. Results and Discussion

3.1. Emission Studies. LIBS spectra of textile dyes were captured from the plasma generated in ambient air using the fundamental harmonic (1064 nm) of a pulsed Nd:YAG laser. The emission spectra were recorded in the optical range of 220 to 700 nm, through a multiple-channel spectrometer. The detector was positioned perpendicularly to the direction of plasma plume expansion at a distance of about 1/2 mm from the sample surface, and spectra were recorded at an average of 20 laser shots to improve the signal-to-noise ratio (SNR). Representative emission spectrum of Sample 1 is shown in Figures 2(a)–2(c).

The spectrum shows a large number of well-separated emission lines having low background. Attentive investigation of this spectrum with the atomic spectral database of NIST (National Institute of Standards and Technology) declares the existence of Al, Ca, Cr, Cu, Fe, K, Mg, Mn, Na, Ni, and Zn. Furthermore, the analysis was confirmed when the LIBS spectra of textile dyes were compared with the individual LIBS spectra of the authentic elements.

3.2. Quantitative Measurements. The concentration of an analyte in a sample can be determined by preparing the standard samples of all the elements of interest in the target. Plotting a calibration curve between known concentrations against the LIBS signal intensities yields the relative composition of the respective elements [19–22]. To calculate the percentage composition of toxic and other elements present in textile dyes, we used three calibration approaches. In the first approach, calibration curves were drawn between known concentrations of the detected elements versus signal intensity. The spectroscopic parameters of the lines used are tabulated in Table 2.

These specific atomic emission lines were selected for being more intense, isolated, and well resolved atomic transition lines in the spectral region. About 99.99% pure fine ground forms of all of the above elements were acquired. To construct the calibration curves, different samples containing stoichiometric ratios of these metals were made. In order to ensure fine mixing and homogeneity, powdered forms of all

Table 2: Spectroscopic data of the lines used for the quantification of detected elements in dyes samples.

Species	Wavelength, λ (nm)	Transition probability, A (s^{-1})	Transitions
Al	309.27	7.29*E*7	$3s^2 3d\ ^2D_{5/2} \rightarrow 3s^2 3p\ ^2P^0_{3/2}$
Ca	643.91	5.3*E*7	$3p^6 4d4p\ ^3F^0_4 \rightarrow 3p^6 3d4s\ ^3D_3$
Cr	425.43	3.15*E*7	$3d^5(^6S)4p\ ^7P^0_4 \rightarrow 3d^5(^6S)4s\ ^7S_3$
Cu	521.82	7.5*E*7	$3d^{10}4d\ ^2D_{5/2} \rightarrow 3d^{10}4p\ ^2P^0_{3/2}$
Fe	259.95	1.47*E*7	$3d^6(^3F_2)4s4p(^3P^0)\ ^5G^0_4 \rightarrow 3d^7(^4F)4s\ ^5F_4$
Mn	383.43	4.29*E*7	$3d^6(^5D)4p\ ^6F^0_{7/2} \rightarrow 3d^6(^5D)4s\ ^6D_{5/2}$
Mg	285.21	4.91*E*8	$3s3p\ ^1P^0_1 \rightarrow 2p^6 3s^{21}S_0$
Ni	336.95	1.8*E*7	$3d^9(^2D)4p \rightarrow 3d^8(^3F)4s^{23}F_4$
Na	588.99	6.16*E*7	$2p^6 3p\ ^2P^0_{3/2} \rightarrow 2p^6 3s\ ^2S_{1/2}$
K	404.72	1.07*E*6	$3p^6 5p\ ^2P^0_{1/2} \rightarrow 3p^6 4s\ ^2S_{1/2}$
Zn	334.50	1.7*E*8	Not Given in NIST database

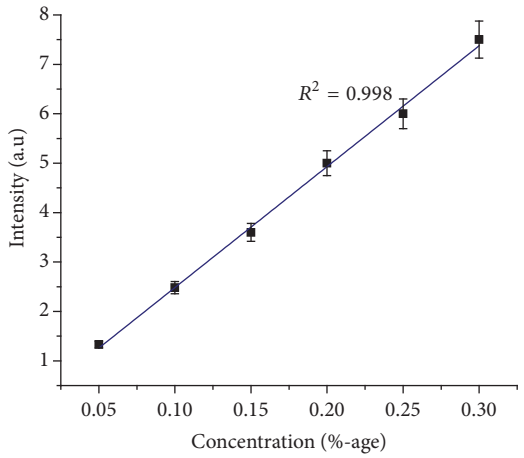

Figure 3: Typical calibration curve for aluminum for Sample 1, yielding the best linear fitting.

of the collected elements were mixed with the matrix material KBr in a ball milling instrument. Four samples of known concentrations, that is, 0.2, 0.15, 0.1, and 0.05%, of elements under study were made in KBr matrix and LIBS spectra were registered for these four concentrations of every element [16].

A typical calibration curve for Al in Sample 1 is shown in Figure 3.

A linear calibration curve with R-squared of 0.998 shows good linear fitting.

The estimated percentage abundance of the species in textile dyes by this method was tabulated in Table 3 and plotted in Figures 4(a)–4(c).

In the second method, the sum of the integrated intensities of all observed emissions (neutral as well as ionized) in the spectra for all elements was utilized to determine the relative abundance of the elements. [23]. The relative concentration of metals in textile dyes through the integrated intensity of all the spectral emissions of an element was tabulated in Table 3 and also shown in Figures 4(a)–4(c).

The third method was calibration-free LIBS. One of the interesting aspects of this technique is that this technique does not require standard samples and involves self-calibration as well. The detailed explanation of this approach can be found in [11, 24, 25]. This procedure is based on the creation and acquirement of emission spectra of an unknown specimen for every element present in the sample and then the calculation of every emission line area [11]. This method needed the following conditions, local thermal equilibrium (LTE), and no self-absorption.

Under the LTE supposition, the transitional intensity of "I" between energy levels E_k to E_i can be expressed as

$$I_\lambda^{ki} = FC_\sigma A_{ki} \frac{g_k}{U_\sigma(T)} e^{(-E_k/kT)}, \quad (1)$$

where C_σ is the abundance of emitting elements, F is called the experimental factor, E_k is the energy, g_k is the statistical weights of the higher level, T gives the average plasma temperature, A_{ki} represents the probability of transition, and U_σ denotes partition function of the emitting elements which is temperature dependent and is given by

$$U_\sigma(T) = \sum_k g_k e^{(-E_k/kT)}. \quad (2)$$

Taking the log of (1) and solving, we readily get

$$q_\sigma = \ln\left(\frac{FC_\sigma}{U_\sigma(T)}\right). \quad (3)$$

That gives the linear relationship as

$$y = mx + q_\sigma, \quad (4)$$

where $x = E_k$, $y = \ln((F \cdot C_\sigma)/U_\sigma(T))$, and $m = -1/kT$.

Using (2), the partition function of each element was measured. The experimental factor F was approximated via the normalization of the sum of the elemental concentrations as follows:

$$\sum_\sigma C_\sigma = \frac{1}{F} \sum_\sigma U_\sigma(T)\, e^{(q_\sigma)} = 1. \quad (5)$$

Table 3: Comparison of LIBS and ICP/AES.

Element	Wavelength (nm)	ICP/AES	LIBS (standard calibration curve method)	CF-LIBS	LIBS (intensities of every emission from every species)
			Sample 1		
Al	309.27	18.0238	17.0241	18.037	20.321
Ca	643.91	23.0335	23.0200	23.500	23.800
Cr	425.43	0.02700	0.02500	0.0200	0.0250
Cu	521.82	0.01600	0.01700	0.2000	0.1250
Fe	259.95	14.8900	14.9000	15.200	14.400
K	404.72	9.32890	9.31900	9.3500	8.7000
Mg	285. 21	11.3297	11.3280	11.389	11.380
Mn	383.43	9.24000	9.30000	10.400	9.7000
Na	588.99	13.3419	13.2000	14.310	15.900
Ni	336.95	1.01600	1.20000	1.5000	1.9000
Zn	334.50	0.02100	0.022000	0.0310	0.0200
			Sample 2		
Al	309.27	13.1330	13.3500	14.200	13.500
Ca	643.91	23.4099	23.9120	23.300	24.450
Cr	425.43	1.00930	1.01000	1.4200	1.9000
Cu	521.82	0.00200	0.00300	0.0090	0.0100
Fe	259.95	10.3170	10.5200	9.4000	11.200
K	404.72	12.0000	12.4000	13.700	12.950
Mg	285. 21	12.2970	12.3000	12.400	12.350
Mn	383.43	10.0459	10.0500	10.180	10.900
Na	588.99	10.0304	10.0200	10.030	11.000
Ni	336.95	2.03900	2.04000	2.6000	2.9000
Zn	334.50	2.54000	2.30000	2.9300	2.7000
			Sample 3		
Al	309.27	20.0208	20.0520	20.900	21.900
Ca	643.91	11.1722	11.3000	10.200	13.000
Cr	425.43	2.11110	2.11900	2.2300	2.3000
Cu	521.82	0.50000	0.59000	0.9000	0.6000
Fe	259.95	14.0170	14.1300	13.000	15.500
K	404.72	11.2350	11.2500	12.900	11.600
Mg	285. 21	10.0640	10.4000	10.090	11.050
Mn	383.43	11.0597	11.0700	14.080	13.060
Na	588.99	11.5500	11.4000	12.700	13.600
Ni	336.95	3.36900	3.57000	3.9000	3.7000
Zn	334.50	1.02200	1.03000	1.7000	2.0000

Hence,

$$F = \sum_{\sigma} U_{\sigma}(T)\, e^{(q_{\sigma})}. \tag{6}$$

q_{σ} (see (4) gives the straight line's intercept of the Boltzmann plot and is related to the logarithm of the abundance of elements times "F." After measuring the value of $U_{\sigma}(T)$, F, and q_{σ}, (3) was used to determine the abundance "C_{σ}" of each species. The relative %-age concentrations of species in target samples via CF-LIBS are shown in Figures 4(a)–4(c) and tabulated in Table 3.

One way to confirm the existence of local thermodynamic equilibrium is to validate for McWhirter criterion:

$$n_e\left(\mathrm{cm}^{-3}\right) \geq 1.6 \times 10^{12} T^{1/2} (\Delta E)^3, \tag{7}$$

where n_e is called the electron density, T is the electron temperature, and ΔE is energy difference between the levels involved in the concerned transition.

In order to determine the degree of ionization and excitation inside the generated plasma, the determination of

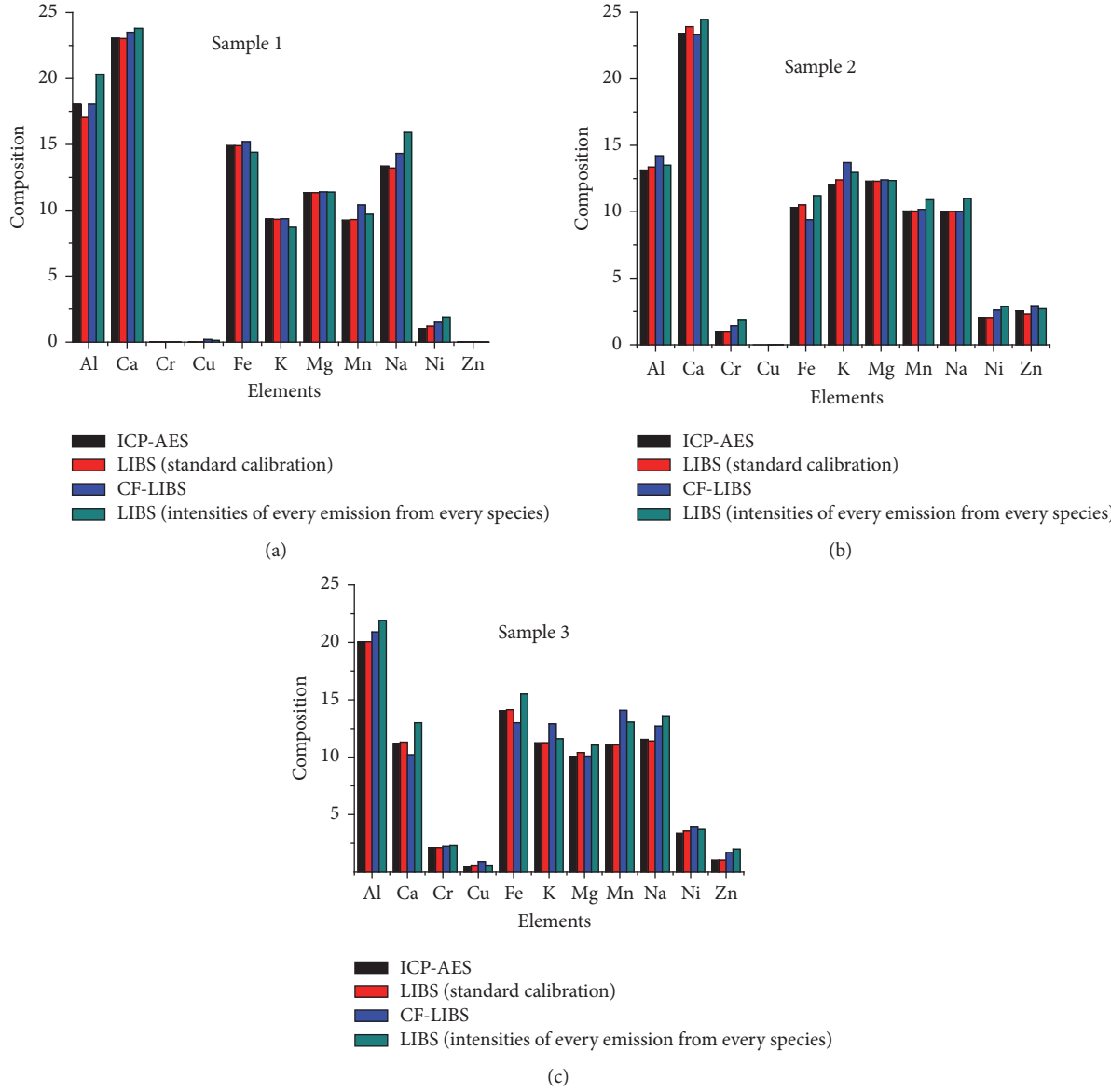

Figure 4: Comparison between the concentrations of toxic and other metals in textile dyes using three LIBS calibration techniques and ICP/AES.

electron number density is mandatory. Stark-broadened line profile of neutral Ca line at 422.67 nm is depicted in Figure 5.

The solid line shows Lorentzian fit, whereas the dotted line points show experimental data. n_e was measured from the full width at half maximum (FWHM) using

$$n_e\left(\mathrm{cm}^{-3}\right) = \left(\frac{\Delta\lambda_{1/2}}{2\omega}\right) \times 10^{16}, \tag{8}$$

where ω stands for the electron impact parameter or Stark-broadening parameter [26]. For Sample 1, the value of the electron density was $(5.4) \times 10^{17}\,\mathrm{cm}^{-3}$ and the electron temperature measured from the Boltzmann plot method was 7849 ± 628 K. By putting the value of electron temperature

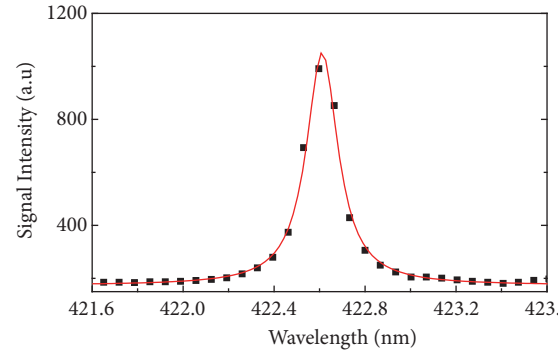

Figure 5: Stark-broadened profile of Ca-I at 422.67 nm with Lorentzian fit.

Table 4: The spectroscopic data of Ca lines used for the determination of electron temperature.

Wavelength, λ (nm)	Transitions	Statistical weight		Transition probability, A (s^{-1})	Excitation energy, E_k (cm^{-1})
		g_k	g_i		
336.19	$3p^6 4s6d\ ^3\mathbf{D}_3 \rightarrow 3p64s4p\ ^3\mathbf{P^0}_2$	7	5	2.23×10^7	45052.374
443.49	$3p^6 4s4d\ ^3\mathbf{D}_2 \rightarrow 3p^6 4s4p\ ^3\mathbf{P^0}_1$	5	3	6.7×10^7	37751.867
445.47	$3p^6 4s4d\ ^3\mathbf{D}_3 \rightarrow 3p^6 4s4p^3\mathbf{P^0}_2$	7	5	8.7×10^7	37757.449
452.69	$3P^6 4snp\ ^1\mathbf{P^0}_1 \rightarrow 3p^6 3d4s\ ^1\mathbf{D}_2$	5	3	4.1×10^7	43933.477
643.91	$3p^6 4d4p\ ^3\mathbf{F^0}_4 \rightarrow 3p^6 3d4s\ ^3\mathbf{D}_3$	7	9	5.3×10^7	35896.889

and ΔE (eV) for the Ca-I line at 422.6 nm in (7), the value that came out was less than the value of electron density calculated using (8). This shows that the dyes generated plasma was in LTE. The electron density was calculated for all the collected samples: Sample 1 ($n_e = 5.8 \times 10^{17}$ cm^{-3}) and Sample 2 ($n_e = 5.3 \times 10^{17}$ cm^{-3}). The measured electron densities were tested for McWhirter criteria and got verified.

For the existence of optically thin plasma, comparisons of the experimentally obtained intensity ratio of two interference-free emission lines with the theoretical intensities were calculated. If the two selected lines have equal upper levels, then the exponential terms vanish and the comparison can be then computed utilizing just the spectroscopic constants [27]. The ratios of Ca-I and Fe-I lines were compared by taking values of their corresponding transition probabilities from the NIST database.

The ratio of Ca-I at 442.5 nm/at 452.6 nm and Ca-I at 649.3 nm/at 646.2 nm and, similarly, the ratio of Fe-I at 440.7 nm/at 441.4 nm and Fe-I at 487.2 nm/at 492.0 nm were determined, and the values obtained on both sides are comparable within ~10% for all the spectra acquired. This consistency reveals the existence of optically thin plasma.

The electron temperature was measured through the Boltzmann plot method using the relative intensities of the detected Ca-I lines. The main equation for the Boltzmann plot method is

$$\ln\left(\frac{I_{ki}\lambda_{ki}}{A_{ki}g_k}\right) = \ln\left(\frac{N(T)}{U(T)}\right) - \frac{E_k}{kT}, \quad (9)$$

where I_{ki} gives the transition intensity between the upper level (k) and lower energy level (i), λ_{ki} is the wavelength of transition, A_{ki} stands for transition probability, g_k stands for statistical weight of upper level (k), $N(T)$ is the upper-level population, $U(T)$ stands for partition function, E_k stands for upper level's energy, k is the Boltzmann constant, and T stands for electron temperature.

The plot of $\ln(\lambda I/gA)$ against energy E_k gives a straight line by just equating the slope of the line to $-1/KT$ which gives the measurement of electron temperature. The graphical representation of Boltzmann plot (Samples 1, 2, and 3) is shown in Figure 6. The spectroscopic parameters of Ca-I emission lines utilized in Boltzmann's plot method are tabulated in Table 4.

The electron temperatures calculated for the emission spectra of the collected samples were given as follows: Sample 2 ($T = 7692 \pm 615$ K) and Sample 3 ($T = 7985 \pm 638$ K).

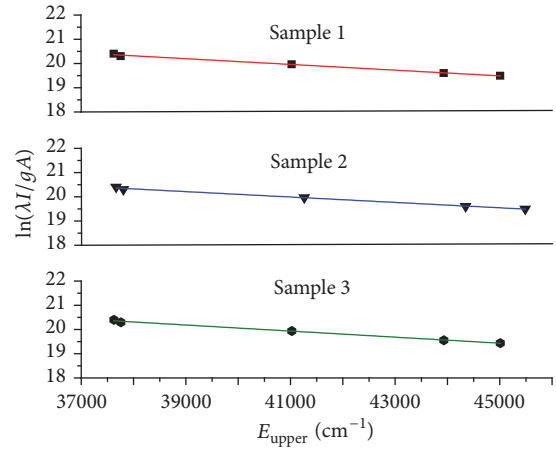

Figure 6: Boltzmann plots for Samples 1, 2, and 3 of textile dyes. The linear fit is represented by a continuous line.

The errors in the electron temperature were due to pulse-to-pulse energy variations and because of uncertainty in the base line selection due to continuum background and interference from adjacent lines. The relative composition of elements calculated through calibration-free LIBS is shown in Figures 4(a)–4(c) along with the relative composition calculated via the integrated intensity methods and ICP/AES.

Usual concentrations of heavy metals in textile dyes are in the following ranges %: 0.0003–0.0083 (Cr), 0.0003–0.0032 (Zn), and 0.0033–0.011 (Cu) [28]. But it was astonishing to find such a huge amount of chromium 2.11900%, nickel 3.57000%, and copper 0.59000% in Sample 3. Zinc (2.30000%) was found to be in an abundant amount in Sample 2. Similarly, Ca was found to be in an abundant amount in all the collected samples. Limits of toxic metals vary and depend upon the amount of heavy metals and degree of contact of textile dyes to consumer's skin. Toxic metals may have different effects on human health such as disorders of the respiratory tract and lung diseases, skin diseases, abnormalities in fertility and pregnancy, and dysfunction of blood and blood producing organs. The extraction of toxic metals from fabrics by perspiration is the main source of the problems. Therefore, textile dyes should be monitored for the presence of different metals (Al, Ca, Cr, Cu, Fe, Mg, Mn, Ni, and Zn) and their existence has to be controlled by applying different production techniques to prevent these health hazards.

In the present study, ICP/AES was utilized as a standard analytical tool. Figures 4(a)–4(c) show the relative concentrations acquired through standard calibration curve technique which were close to the analysis of ICP/AES.

4. Conclusion

Spectroscopic study of textile dyes was carried out by LIBS to determine their composition as well as relative concentrations. The emission spectra revealed the presence of toxic metals (Co, Cr, Cu, Fe, Ni, and Zn) in addition to other elements (Al, Mg, Ca, and Na) in textile dyes. Furthermore, the plasma temperature was determined with a Boltzmann plot method. The electron number density was estimated from Stark-broadened line profiles. The measured electron temperature was the same for all the measured spectra within the range of experimental uncertainty. The comparative analysis of LIBS versus ICP/AES showed that the standard calibration curve method provides the closest results to the results of ICP/AES. Particularly, the amount of zinc and chromium was observed to cross the recommended limit in Sample 2 which may have different effects on human health such as skin allergy. Therefore, it is appreciable to monitor the existence of toxic metals in textile materials. Similarly, the concentrations of toxic metals (chromium and copper) were found to be above the permissible safe limits in Sample 3.

Conflicts of Interest

The authors declare that they have no conflicts of interest.

References

[1] V. Majidi and M. R. Joseph, "Spectroscopic applications of laser-induced plasmas," *Critical Reviews in Analytical Chemistry*, vol. 23, no. 3, pp. 143–162, 1992.

[2] L. J. Radziemski, "Review of selected analytical applications of laser plasmas and laser ablation, 1987–1994," *Microchemical Journal*, vol. 50, no. 3, pp. 218–234, 1994.

[3] M. Sabsabi and P. Cielo, "Quantitative analysis of aluminum alloys by Laser-induced breakdown spectroscopy and plasma characterization," *Applied Spectroscopy*, vol. 49, no. 4, pp. 499–507, 1995.

[4] C. M. Davies, H. H. Telle, D. J. Montgomery, and R. E. Corbett, "Quantitative analysis using remote laser-induced breakdown spectroscopy (LIBS)," *Spectrochimica Acta Part B: Atomic Spectroscopy*, vol. 50, no. 9, pp. 1059–1075, 1995.

[5] O. Samek, D. C. S. Beddows, J. Kaiser et al., "Application of laser-induced breakdown spectroscopy to in situ analysis of liquid samples," *Optical Engineering*, vol. 39, no. 8, pp. 2248–2262, 2000.

[6] H. H. Telle, D. C. S. Beddows, G. W. Morris, and O. Samek, "Sensitive and selective spectrochemical analysis of metallic samples: the combination of laser-induced breakdown spectroscopy and laser-induced fluorescence spectroscopy," *Spectrochimica Acta Part B: Atomic Spectroscopy*, vol. 56, no. 6, pp. 947–960, 2001.

[7] Y. Yoon, T. Kim, M. Yang, K. Lee, and G. Lee, "Quantitative analysis of pottery glaze by laser induced breakdown spectroscopy," *Microchemical Journal*, vol. 68, no. 2-3, pp. 251–256, 2001.

[8] O. Samek, D. C. S. Beddows, H. H. Telle, G. W. Morris, M. Liska, and J. Kaiser, "Quantitative analysis of trace metal accumulation in teeth using laser-induced breakdown spectroscopy," *Applied Physics A*, vol. 69, no. 1, pp. S179–S182, 1999.

[9] P. Fichet, P. Mauchien, J.-F. Wagner, and C. Moulin, "Quantitative elemental determination in water and oil by laser induced breakdown spectroscopy," *Analytica Chimica Acta*, vol. 429, no. 2, pp. 269–278, 2001.

[10] R. Barbini, F. Colao, R. Fantoni, A. Palucci, and F. Capitelli, "Application of laser-induced breakdown spectroscopy to the analysis of metals in soils," *Applied Physics A: Materials Science and Processing*, vol. 69, no. 7, pp. S175–S178, 1999.

[11] I. Rehan, K. Rehan, S. Sultana, M. O. ul Haq, M. Z. K. Niazi, and R. Muhammad, "Spatial characterization of red and white skin potatoes using nano-second laser induced breakdown in air," *The European Physical Journal Applied Physics*, vol. 73, no. 1, article 10701, 2016.

[12] O. Samek, D. C. S. Beddows, H. H. Telle et al., "Quantitative laser-induced breakdown spectroscopy analysis of calcified tissue samples," *Spectrochimica Acta Part B: Atomic Spectroscopy*, vol. 56, no. 6, pp. 865–875, 2001.

[13] L. Hong-kun, L. Ming, C. Zhi-jiang, and L. Run-hu, "LIBS elemental analysis in aluminum alloy using fundamental beam from Nd: YAG laser (1064 nm)," *Transactions of Nonferrous Metals Society of China*, vol. 18, pp. 222–226, 2008.

[14] V. K. Singh, N. K. Rai, S. Pandhija, A. K. Rai, and P. K. Rai, "Investigation of common Indian edible salts suitable for kidney disease by laser induced breakdown spectroscopy," *Lasers in Medical Science*, vol. 24, no. 6, pp. 917–924, 2009.

[15] M. A. Gondal, M. M. Nasr, M. M. Ahmed, Z. H. Yamani, and M. S. Alsalhi, "Detection of lead in paint samples synthesized locally using-laser-induced breakdown spectroscopy," *Journal of Environmental Science and Health, Part A*, vol. 46, no. 1, pp. 42–49, 2011.

[16] T. Hussain and M. A. Gondal, "Laser induced breakdown spectroscopy (LIBS) as a rapid tool for material analysis," *Journal of Physics: Conference Series*, vol. 439, no. 1, article 012050, 2013.

[17] M. Dell'Aglio, R. Gaudiuso, G. S. Senesi et al., "Monitoring of Cr, Cu, Pb, v and Zn in polluted soils by laser induced breakdown spectroscopy (LIBS)," *Journal of Environmental Monitoring*, vol. 13, no. 5, pp. 1422–1426, 2011.

[18] A. Khalid, S. Bashir, M. Akram, and A. Hayat, "Laser-induced breakdown spectroscopy analysis of human deciduous teeth samples," *Lasers in Medical Science*, vol. 30, no. 9, pp. 2233–2238, 2015.

[19] M. A. Gondal, M. A. Dastageer, F. F. Al-Adel, A. A. Naqvi, and Y. B. Habibullah, "Detection of highly toxic elements (lead and chromium) in commercially available eyeliner (kohl) using laser induced break down spectroscopy," *Optics and Laser Technology*, vol. 75, pp. 99–104, 2015.

[20] W. T. Y. Mohamed, "Improved LIBS limit of detection of Be, Mg, Si, Mn, Fe and Cu in aluminum alloy samples using a portable Echelle spectrometer with ICCD camera," *Optics and Laser Technology*, vol. 40, no. 1, pp. 30–38, 2008.

[21] B. Bousquet, J.-B. Sirven, and L. Canioni, "Towards quantitative laser-induced breakdown spectroscopy analysis of soil samples," *Spectrochimica Acta Part B: Atomic Spectroscopy*, vol. 62, no. 12, pp. 1582–1589, 2007.

[22] M. A. Gondal, T. Hussain, and Z. H. Yamani, "Optimization of the LIBS parameters for detection of trace metals in petroleum products," *Energy Sources A*, vol. 30, no. 5, pp. 441–451, 2008.

[23] M. Qasim, M. Anwar-ul-Haq, M. Sher Afgan, M. A. Kalyar, and M. A. Baig, "Elemental Analysis of Black Salt by Laser-Induced Breakdown Spectroscopy and Inductively Coupled Plasma–Optical Emission Spectroscopy," *Analytical Letters*, vol. 49, no. 13, pp. 2108–2118, 2016.

[24] M. Dell'Aglio, A. De Giacomo, R. Gaudiuso, O. D. Pascale, G. S. Senesi, and S. Longo, "Laser Induced Breakdown Spectroscopy applications to meteorites: Chemical analysis and composition profiles," *Geochimica et Cosmochimica Acta*, vol. 74, no. 24, pp. 7329–7339, 2010.

[25] T. Takahashi, B. Thornton, K. Ohki, and T. Sakka, "Calibration-free analysis of immersed brass alloys using long-ns-duration pulse laser-induced breakdown spectroscopy with and without correction for nonstoichiometric ablation," *Spectrochimica Acta Part B: Atomic Spectroscopy*, vol. 111, pp. 8–14, 2015.

[26] H. R. Griem, *Plasma spectroscopy, Chap. 6*, McGraw-Hill, New York, NY, USA, 1964.

[27] L. Radziemski and D. Cremers, "A brief history of laser-induced breakdown spectroscopy: From the concept of atoms to LIBS 2012," *Spectrochimica Acta Part B: Atomic Spectroscopy*, vol. 87, pp. 3–10, 2013.

[28] S. Barclay and C. Buckley, "*Waste Minimization Guide for the Textile Industry," A Step Towards Cleaner Production*, vol. 1, 2000.